

An x-ray biplanar photodiode and the x-ray emission from magnetically confined laser produced plasma

V N RAI, M SHUKLA and H C PANT

Laser Plasma Laboratory, Centre for Advanced Technology, Indore 452 013, India
Email: vnrai@cat.ernet.in; Fax: 91-731-488430

MS received 27 August 1997; revised 3 August 1998

Abstract. Development of a single and multichannel biplanar vacuum photodiode for x-ray detection is reported, which has been used to study the x-ray emission from laser produced plasma expanding across an externally applied magnetic field. Two to three times enhancement in x-ray emission has been observed which was found correlated with decrease in size of the x-ray emitting plasma plume (expansion velocity of plasma). Experimental observations were found in close agreement with the analytical model based on an increase in plasma density as a result of plasma confinement in magnetic field. Temporal evolution of x-ray emission indicates that recombination radiation seems to be playing an important role in x-ray enhancement.

Keywords. Biplanar vacuum photodiode; x-ray emission; laser plasma; magnetic field.

PACS Nos 52.70; 52.25; 52.40

1. Introduction

X-ray measurements are being used as an important diagnostic [1] for studying high temperature plasma particularly in the inertially confined (laser produced plasma) [2] as well as magnetically confined fusion (Tokamak) research. Rapidly time varying hydrodynamic and radiative processes in laser produced plasma experiments demand detailed studies of time resolved x-ray emission from laser produced plasma. X-ray streak camera, x-ray framing camera, gated microchannel plate and silicon photodiodes [1–2] have been used as a detection system to study the time dependent x-ray emission. X-ray streak camera, framing camera and gated microchannel plate have various other advantages but involve very complicated electronics along with high price and difficulty in procurement. Silicon photodiodes have nonlinear response with x-ray energy and get saturated at comparatively low x-ray flux. Vacuum photodiode is free from all these problems and has easy fabrication technique. Many designs of vacuum photodiodes [3–6] have been reported in literature with a time response varying from 60 to 450 ps but with a complicated design. We are reporting in this paper the development of a low cost single and multichannel vacuum photodiode

[7–8] which has been used to study the x-ray emission from a magnetically confined laser produced plasma. There is a large interest in the generation of a short time duration intense and small size x-ray source for various applications [1] such as plasma diagnostics in the field of thermonuclear research particularly in inertial confinement fusion as a backlighting source, x-ray laser, x-ray lithography, x-ray microscopy and EXAFS etc. This type of x-ray source can be obtained from laser produced plasma (LPP) using a short time duration high intensity laser. Enhancement in x-ray intensity is limited at high intensity of laser due to the generation of various parametric instabilities [9–10] which produce hot electrons in the plasma. X-ray intensity increases [11] as the wavelength of the laser decreases due to increase in critical density as a result of an efficient laser absorption in the plasma. Along with the use of high Z material as a target to enhance the x-ray emission, various other techniques have also been tried and reported in the literature, firstly an oblique incidence [12] of laser which increases the resonance absorption of laser in the plasma, secondly the confinement of laser produced plasma in various types of gold cavity [13–14]. An interesting technique has been used by Suckewer *et al* [15–16] to enhance the gain of x-ray laser by confining the plasma column in a strong solenoidal magnetic field and cooling it by radiation loss. An enhancement of ~ 100 in stimulated emission over spontaneous emission of the C VI 182 Å line was measured in the presence of a confining magnetic field of 90 KG. He has compared the x-ray emission along and perpendicular to the magnetic field but no information was given about the emission with and without magnetic field. An other experiment performed by Enright and Burnett [17] using CO₂ laser at 100 KG confining magnetic field have shown an enhancement in hard x-rays (100–200 keV) along with the generation of hot electrons. All the above experiments were performed in a condition where confining magnetic field and plasma temperature were very high. However many points are still unanswered such as the process of x-ray emission, enhancement and characteristics of x-rays emitted in the presence of low magnetic field and plasma temperature where plasma β is nearly comparable to the high magnetic field experiments after expansion. Its behaviour with the other plasma parameters such as ambient chamber pressure.

The main aim of the present paper is to report the design of a simple single and multi-channel (four) vacuum photodiode and a comprehensive study of x-ray emission from laser produced plasma when plasma temperature and magnetic field are low. The result of x-ray enhancement is correlated with the ion expansion velocity as well as with the result reported by Enright and Burnett [17] where experiment was performed at high plasma temperature (10–15 keV) as well as a magnetic field (100 k gauss) using CO₂ laser. In this experiment plasma was expanding across the externally applied uniform magnetic field (0.6T). The effect of ambient pressure on the x-ray emission with and without magnetic field is also discussed.

2. Vacuum photodiode

2.1 Theory

Before describing the design of biplanar photodiode, it is important to understand the physical process taking place inside the photodiode, when an ultraviolet or x-ray photon interacts with the photocathode. Figure 1a shows the schematic diagram of a photodiode. Interac-

Magnetically confined laser produced plasma

tion of photons with photocathode releases electrons without any delay whose energies are decided by the wavelength of the incident photons. Due to a biasing voltage (V_b) present inbetween photocathode and anode, an electric field $E = V_b/d$ accelerates the electron towards the anode, where d is separation between electrodes. In the case of uniform electric field electron velocity rises linearly with the time t . The rate of change of charge induces current in the circuit proportional to the electron velocity. The current induced by a single electron can be given by

$$I = eV, \quad (1)$$

where e is the electronic charge and V is the velocity of electron in electric field, which can be expressed as

$$V = (eV_b/m_e) \cdot T \quad 0 < T < T_r, \quad (2)$$

where m_e is the mass of the electron. Equations 1 and 2 clearly indicate that current rises linearly with time till electron reaches at anode after travelling distance d in time T_r . The expression for T_r can be written with the help of eq. (2) as

$$T_r = d(2m_e/e)^{1/2} \cdot V_b^{-1/2} = 2.7 \times 10^{-6} d/V^{1/2}. \quad (3)$$

The maximum value for I can be given by

$$I_{\max} = (2e^3/m_e)^{1/2} \cdot V_b^{1/2}. \quad (4)$$

Equations 3 and 4 indicate that rise time is inversely proportional to the square root of the applied voltage between the electrodes, whereas peak current is directly proportional to the square root of biasing voltage. This means that higher biasing voltage is important for both rise time as well as induced signal. Figure 1b shows the equivalent circuit for the vacuum photodiode in which induced current flow through the capacitor formed due to interelectrode separation and a load resistance R_L . V_S signal thus generated across load R_L rises during the electron flight time to its maximum value (V_{SO}) and then decays exponentially with a time constant $\tau = R_L C$ which can be expressed as

$$V_S = V_{SO} \exp[-(T - T_r)/\tau] \quad T > T_r, \quad (5)$$

which indicates that the fall time of the induced signal is limited by the discharge time constant of capacitor formed due to interelectrode separation. It has been reported [3] that space charge limitation in photodiode does not affect the response of the photodiode. The combination of the above equations are capable of describing the response of the photodiode for a given parameter and incident photon flux of any wavelength.

2.2 Design

2.2.1 Single channel vacuum photodiode: Figure 1 shows the schematic diagram of a single channel biplanar vacuum photodiode [7]. It consists of a combination of grid and photocathode (dia ~ 20 mm). The grid has $\sim 80\%$ transmission and forms the high voltage electrode of diode which was placed on a brass ring separated from photocathode by a teflon annular ring of thickness (0.5–1mm). The grid was connected to high voltage through an

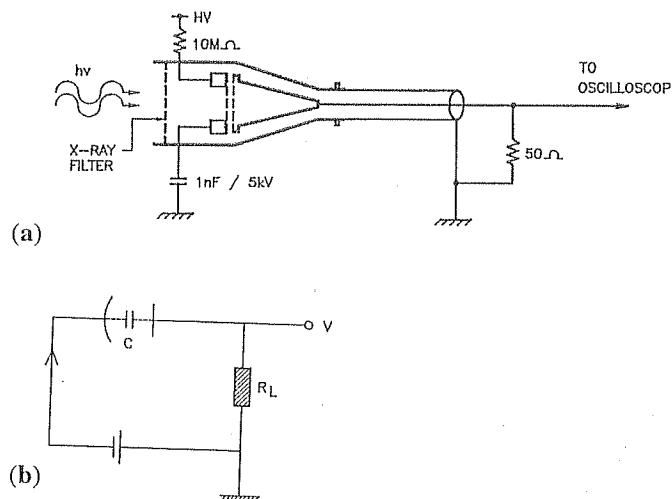
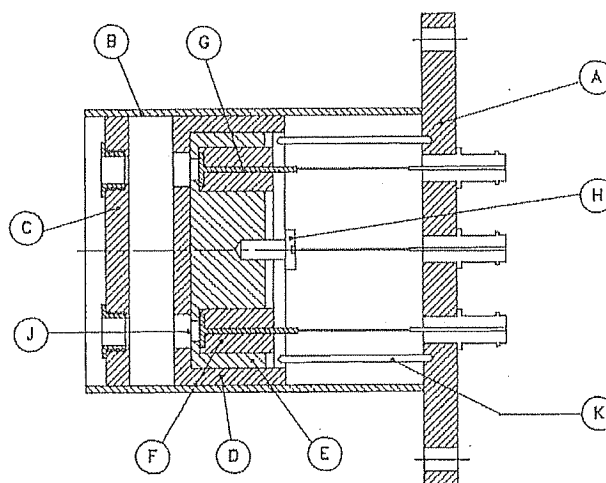


Figure 1. (a) Schematic diagram of single channel vacuum photodiode. (b) Equivalent circuit of photodiode.

isolating resistance of $10\text{ M}\Omega$. A $1\text{ nF}/5\text{ kV}$ ceramic capacitor was connected between grid and ground to improve the low frequency response of the diode whereas high frequency response of the diode is limited by the transit time of photoelectrons between photocathode and grid as well as by the stray inductance present in the circuit. The photocathode as well as the grounded housing of the diode has a conical geometry as shown in figure 1 to match with the $50\ \Omega$ BNC connector from where the output signal was taken out. Outer housing was made out of brass whereas the photocathodes were made out of aluminum and gold plated copper. The surface finish of photocathode should be such as to provide long term stability in quantum efficiency because rough surfaces encourage oxidation. An arrangement was made to put an x-ray filter attached on an annular teflon ring in front of the grid to select the spectral range of the x-rays being detected. An output signal was recorded across $50\ \Omega$ from the photocathode using a fast oscilloscope to avoid the reflection of signals. However to improve the S/N ratio of the diode one can increase the sensitivity of detector either by increasing the area of photocathode or by increasing the value of termination resistance at the cost of time response of the detector.

2.2.2 Multichannel vacuum photodiode: Figure 2 shows the schematic diagram of multichannel vacuum photodiode [8] which consists of four vacuum photodiodes in one assembly. Only difference in this case is that photocathode has a disc of $\sim 10\text{ mm}$ diameter and a pin coming out from the disc which makes $50\ \Omega$ geometry with the common metal housing for all the four photodiodes. However, a mismatch remains between the photocathode pin and BNC connector near the electrical joints This photodiode was operated in two mode, in one case voltage was applied on the grid and the signal was taken from the cathode across



- | | |
|-------------------|------------------|
| A : SS Flange | F : Teflon cap |
| B : SS Housing | G : Photocathode |
| C : Filter Holder | H : Brass screw |
| D : Nylon cap | J : Grid |
| E : SS Holder | K : Brass Holder |

Figure 2. Schematic diagram of multichannel vacuum photodiode.

50 Ω termination whereas in the other case voltage was applied on the photocathode and the grid was grounded where output signal from the photocathode was taken through a capacitor to isolate the DC voltage coming on the input of the oscilloscope. X-ray signals were recorded using multichannel photodiode in different energy range in single shot by using different types of x-ray filters in front of grids of the photodiodes. Both the systems were assembled with the flange of vacuum chamber with a vacuum tight feed through which is provided the output signal.

3. Experiment

The experimental setup used in the present study consists of a 35 picosecond time duration Nd:YAG laser (75 mJ) operating in second harmonics at 0.53 μm delivering up to 15 mJ energy in ~ 25 ns time duration. The laser beam was focused onto the copper target using a spherical lens of 30 cm focal length. Laser energy was changed using neutral density filters. Thick planar targets of copper, aluminum and gold were used to form the plasma in a vacuum chamber evacuated at $\sim 10^{-5}$ torr pressure. The x-rays emitted from laser produced plasma were used to test the single channel and multichannel vacuum photodiode

[7–8]. A thin zapon ($4\ \mu\text{m}$) and $12\ \mu\text{m}$ aluminum foil were used as a filter in front of the photodiodes. X-ray detectors were kept at 45° with respect to the target normal whereas two Langmuir probes were kept at $\sim 10^\circ$ (just below the laser beam) and 45° with respect to the target normal at a radial distance of 5 and 17 cm respectively to monitor the ion saturation current. The electrical signals from the x-ray vacuum photodiodes and the Langmuir probes were recorded using a 100 MHz L & T Gould model 7074 digital storage oscilloscope (400 MS/S). X-ray pin hole and streak camera [18–19] were also used to get spatial and temporal evolution of x-ray emission from laser produced plasma in the absence and presence of magnetic field. Two bar magnets of 10×10 mm cross-sectional area, kept at 5 mm separation, were used to generate an uniform magnetic field of ~ 0.6 T between the poles to see the effect of magnetic field on x-ray emission when the plasma was expanding across it. Both the target and the bar magnets were held inside the plasma chamber with the help of two independent manual manipulators such that the target was inbetween the magnetic poles. Position of the target was changed without affecting the magnetic field at the location of plasma formation, so as to take each shot at a fresh location. Laser plasma produced in this arrangement expands ~ 3 mm in uniform magnetic field of 0.6 Tesla. But as the plasma comes out of the magnetic poles it passes through a decreasing magnetic field because of increasing distance from the magnetic pole. Arrangement was made to pull the magnet in such a way that it remains inside the chamber but plasma can be generated in the absence of a magnetic field. However, a residual magnetic field of ~ 100 G was measured at the target location when the magnet was away from the location of plasma formation.

4. Results and discussion

4.1 Testing of vacuum photodiode

Figure 3 shows the oscillogram of the signal obtained from a single channel vacuum photodiode when x-rays fall on its photocathode [7]. The picosecond laser signal recorded using PIN-photodiode is also shown for comparison in the same oscillogram. Both the signals have similar rise time, nearly ~ 1 ns, which is limited by the sampling rate of oscilloscope (1G sample, Lecroy model 9350 A). A fast oscilloscope is needed to record the subnanosecond phenomenon because the calculated response time of the photodiode is T_r (10% to 90%) = $0.8d(2m_e/eV_b)^{1/2} \cong 130$ ps for a biasing voltage of 100 volts and electrode separation of 0.5 mm. It is necessary to have a fast oscilloscope if the temporal response of x-ray emission is to be recorded in picosecond regime using this type of photodiode. Otherwise it will provide time independent integrated information. Figure 4 shows the oscillogram of three photodiode signals from multichannel photodiode assembly. Out of three traces, the first one (a) was recorded with a photodiode without any filter whereas rest of the two traces (b) & (c) were recorded in the presence of $\sim 4\ \mu\text{m}$ thick Zapon as well as $12\ \mu\text{m}$ thick aluminum filter respectively. In the former case detector was sensitive for ultraviolet as well as x-rays which remain for a longer time > 20 ns, whereas in the latter case (presence of Zapon and aluminum filter) it is sensitive for soft as well as hard x-rays which shows time duration of the pulse as ~ 3 ns which is again limited by the oscilloscope sampling rate (L&T Gould model 7074). Time duration of UV and x-ray emission recorded using photodiodes are found in agreement with the measurement made using streak camera [19] where ultraviolet and x-rays last for > 20 ns (without filter) and soft x-ray lasts for

Magnetically confined laser produced plasma

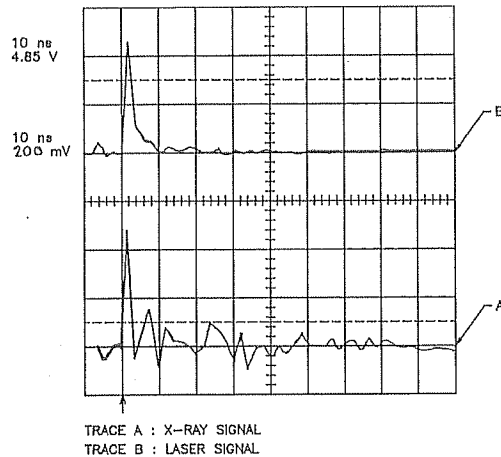


Figure 3. Oscilloscope of single channel vacuum photodiode signal.

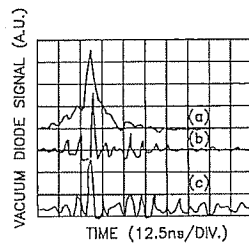


Figure 4. Oscilloscope of multichannel vacuum photodiode signal.

1.5 ns (with Zapon filter). During this experiment photodiodes were biased to ~ 700 volts and signals were recorded across 50Ω termination. In figure 4 one can notice the presence of two smaller peaks before the main peak for all the photodiode records. These pulses are due to the presence of two mode locked pre-pulses before the main laser pulse separated by 7 ns time duration. These multiple mode locked pulses were noticed when acoustooptic modulator of the picosecond laser was not properly aligned. However during best alignment case also, one can see two smaller laser pulses before and after the main laser pulse separated by 7 ns. Important observation in this case was that the main x-ray signal increases when two prepulses were present with a significant amplitude which can generate plasma before the main laser pulse. But comparatively less x-ray signal was noticed when only one laser pulse with smaller side bands are present during best alignment of laser. This indicates that expanded plasma formed during prepulse interact with the main laser pulse and provides a good condition for laser light absorption in plasma corona as well as plasma heating and consequently an increase in x-ray emission. These photodiodes were used to study the x-ray emission from laser produced plasma expanding across an uniform magnetic field. In this experiment, photodiode signals were recorded across $1 M\Omega$, that is, in

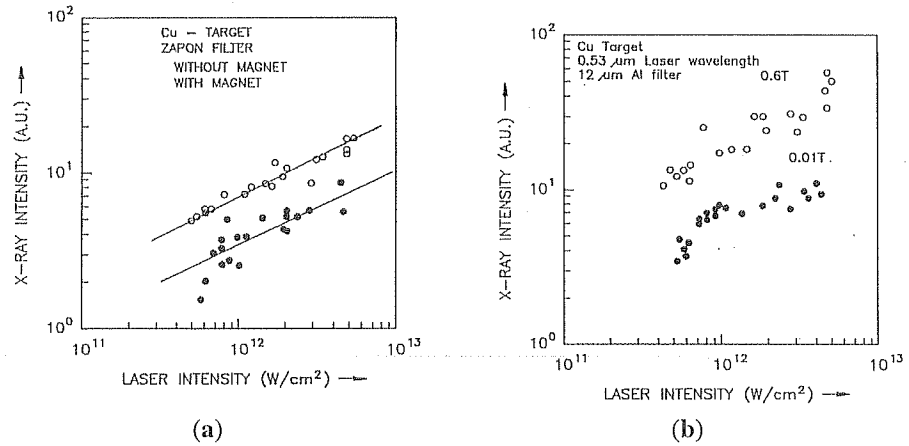


Figure 5. Variation of x-ray emission with laser intensity in the presence (0.6T) and absence (0.01T) of magnetic field. (a) With Zapon filter. (b) With 12 μm Al filter.

the integration mode due to two reasons. First to increase the signal generated due to x-rays and secondly to avoid the fluctuations in photodiode signal due to sampling and reflection as a result of impedance mismatch. The peak amplitude of integrated signal was considered as x-ray signal in arbitrary unit during this experiment. However temporal response of x-ray emission was recorded using x-ray streak camera.

4.2 Study of x-ray emission

Figure 5a shows the variation of x-ray signal with laser intensity in the presence and absence of magnetic field. It was observed that the x-ray signal from copper plasma got enhanced by 2–3 times in the presence of magnetic field (0.6 T) as compared to the x-ray signal in the absence of the magnetic field [20]. However, enhancement was ~ 3 –4 times in the case of gold and ≤ 2 times in aluminum plasma. In this case x-ray detector with zapon filter was sensitive for soft as well as hard x-ray energy. Figure 5b shows variation of x-ray emission with laser intensity when another detector has a 12 μm thick aluminum filter which is transparent mainly for x-rays with energy $E > 2$ keV. All the above measurements at 0.6 T magnetic field were compared to the signal obtained in the absence of magnetic field (residual magnetic field of 0.01 T). However, there was no observable change in the x-ray signal in the presence of 0.01 Tesla magnetic field than in the absence of magnetic field. It seems from figure 5b that the enhancement is ~ 4 to 5 times more, towards the higher intensity side ($\sim 5 \times 10^{12}$ W/cm²). However, it was not possible to go beyond this intensity range due to experimental limitations. Similar enhancement in high energy x-rays ($E > 100$ keV) in the presence of magnetic field has been observed earlier [17]. The scaling of x-ray emission with laser intensity follows the power law variation as $I_X \propto (I_L)^\alpha$ with $\alpha = 0.5$ which is less in comparison to the value of $\alpha \sim 1.5 - 2$ measured in the absence of magnetic field [8,21]. The spread in data in the case of 0.01 T magnetic field has (figure 5a and 5b) two slopes in comparison to one slope ($\alpha \sim 0.5$) observed in the case of high magnetic field. Initially the slope was $\alpha \sim 1.5$ up to intensity range $\sim 10^{12}$ W/cm² but it goes

down ($\alpha = 0.5$) for the laser intensity above $\sim 10^{12}$ W/cm² which is similar to the slope obtained in the case of 0.6 T magnetic field. This experiment was repeated many times and the observations were found reproducible. These observations indicate that at 100 G magnetic field a new decreased slope develops after a certain laser intensity as the intensity increases. However only one decreased slope ($\alpha \sim 0.5$) is seen at higher magnetic field of 0.6 T for all the experimental ranges of intensity. It seems that threshold intensity is very small (out of experimental range) in the case of 0.6 Tesla magnetic field which indicates that the threshold intensity where slope changes may be dependent on the magnetic field and it decreases with an increase in the magnetic field. This is an indication that the absorbed laser energy is being lost through a new channel which is dependent on the strength of magnetic field as well as on the laser intensity. In this case, part of the absorbed laser energy seems to be lost in generating the high frequency (~ 100 MHz) instabilities which are observable on ion current signal measured using Langmuir probe as well as in x-ray pin hole pictures. Generation of similar kind of instability known as finite larmor radius instability has been reported earlier when the plasma was decelerated by a magnetic field [22]. Chang and Hasmi [23] have reported that even the presence of ~ 170 G magnetic field can generate fluctuation in ion current which is similar to our case. The presence of instabilities in the plasma creates energy loss through the enhanced particle flux outside the plasma as a result of wave particle interaction. A detailed study of oscillation modes in the plasma expanding across the magnetic field will be reported separately.

Figure 6a shows the ion current measured in the absence of magnetic field by a Langmuir probe located at ~ 15 cm radial distance from the target and at 45° from the target normal. The expansion velocity of ions was calculated as $\sim 1.4 \times 10^7$ cm/s at the peak of the ion current. X-ray signal on the probe was considered as reference for calculating the time of flight of ions. Figure 6b shows the ion saturation current when the plasma was expanding across an uniform magnetic field (0.6 T). Two main peaks along with some oscillations are seen in the ion current. It was noted that amplitude of the ion current pulse goes down in the presence of magnetic field along with an increase in its FWHM. The expansion velocity in the case of first peak comes out to be $\sim 1.13 \times 10^7$ cm/s in comparison to $\sim 1.42 \times 10^6$ cm/s for the second peak. The number of peaks in the ion current in figure 6b seems to be due to the number of bounce taken by ions on the plasma and magnetic field line interface. Oscillations are damped in nature as a result of finite plasma resistance, as has been observed experimentally [24] and reported theoretically earlier [25]. The ions expanding across the magnetic field gets decelerated due to which the expansion velocity of the first peak (during first bounce) goes down by 20% whereas in the second peak case (during second bounce) velocity remains 17% of the expansion velocity measured in the absence of the magnetic field. A drastic decrease in expansion velocity during second peak seems to be due to cooling effect in the plasma. Figure 6c shows multiple bounce of plasma when it was expanding ~ 10 mm across uniform magnetic field. Observation of multiple peak in ion current indicates that magnetic field lines oscillates under the effect of plasma pressure and restoring force due to magnetic pressure. Initially smooth expansion takes place when $\beta \gg 1$ whereas first bounce in plasma expansion occur near $\beta = 1$ surface where plasma pressure is equal to the magnetic pressure [24–25]. In the case when plasma is perfectly conducting, ion current will oscillate without damping. The bouncing radius (R_b) of the plasma in the presence of magnetic field was calculated using the following

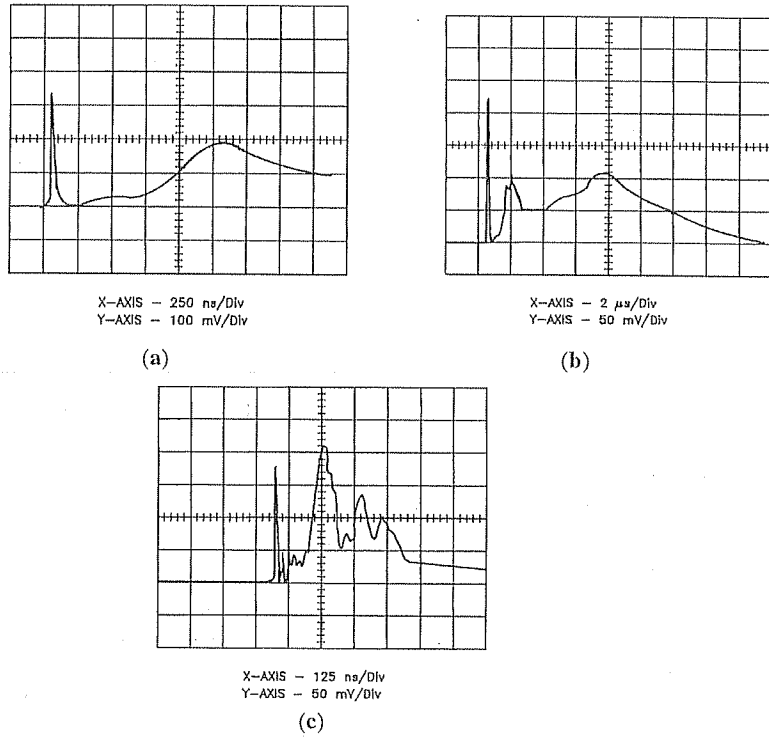


Figure 6. Time of flight signal of ions measured using Langmuir probe (a) In the absence of magnetic field; (b) In the presence of magnetic field (0.6T) at $r = 15$ cm, $\theta = 45^\circ$; (c) In the presence of magnetic field (0.6T) at $r = 5$ cm, $\theta = 10^\circ$ below the laser beam.

relation [24].

$$R_b = \frac{9}{2} \left[\frac{NkT_e}{B^2} \right]^{1/3}, \quad (6)$$

where $B = 6$ KG and $N \sim 1.36 \times 10^{14}$ is the total number of plasma particles present in the plasma volume which was calculated on the basis of scaling law for mass ablation rate. The plasma temperature was measured to be $kT_e \sim 180$ eV using K -edge spectrometer which according to eq. (1) provided $R_b \sim 1698 \mu\text{m}$. The plasma bounce time $\sim R_b/V \sim 30$ ns was calculated on the basis of measured plasma expansion velocity. Accordingly plasma deceleration was found to be $\sim 4.67 \times 10^{14} \text{ cm/s}^2$, according to which plasma expansion velocity goes down by 1.66% after 500 ps, which indicates that magnetic field starts confining the plasma after 500 ps. However, confinement of plasma was confirmed by recording the pin hole pictures of x-ray emitting plasma plume in the absence and presence of magnetic field (figure 7). It was noted that x-ray emitting plume expands up to 450 and 350 μm in the absence and presence of magnetic field, respectively. Decrease in the size of plume in the presence of magnetic field is due to the confinement of plasma, which will

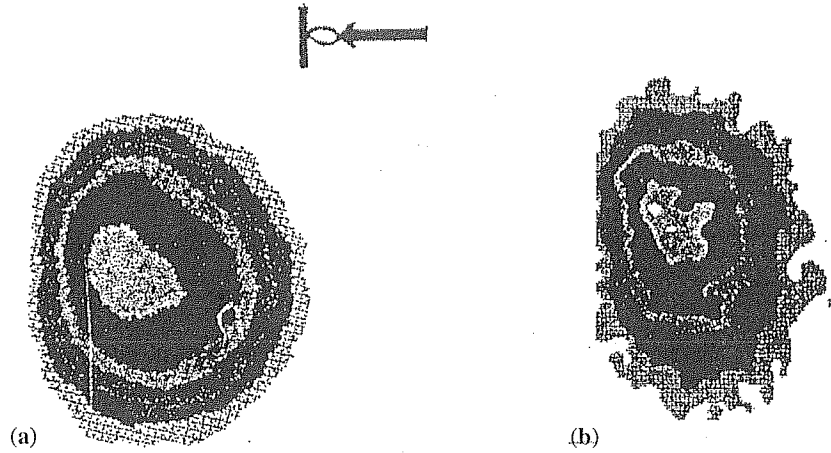


Figure 7. X-ray pinhole pictures of x-ray emitting plume. (a) In the absence of magnetic field. (b) In the presence of magnetic field.

increase the effective plasma density in the decreased volume of x-ray emitting plume. A comparison of pin hole pictures shows that plasma expansion does not remain smooth in the presence of magnetic field. Distortion was seen at each iso-intensity contour (figure 7b) which indicates the presence of instability in the plasma as a result of plasma deceleration in the magnetic field. Probably these are the same instabilities observed on the ion saturation current signal and discussed earlier.

Figures 8a and 8b show the temporal evolution of x-ray emission in the absence and presence of magnetic field. It shows that the time duration of x-ray emission remains same (1.5 ns) in both the cases whereas FWHM increases in the presence of magnetic field. The main increase in x-ray emission takes place after ~ 500 ps, that is, after peak of x-ray emission. This shows that increase in x-ray intensity took place when plasma expanded away from the target surface and as a result started cooling ($kT_e \propto 1/r^2$, where r is distance from critical surface). As the plasma temperature goes down possibility of recombination radiation ($\propto 1/T^{3/2}$) may go up in comparison to the Bremsstrahlung ($\propto 1/T^{1/2}$) and the line radiation ($\propto 1/T^{1/2}$). However, x-ray spectroscopic data are needed to confirm the dominance of recombination radiation for which diagnostics are in developmental stage. An increase in effective density as a result of confinement will also add up in enhancing the x-ray emission. However, these effects will be common for all the three processes of x-ray emission ($\propto \text{NiNe}$). An enhancement in x-ray emission during deceleration of plasma may be possible either due to conversion of kinetic energy of plasma into the thermal energy or due to enhancement in recombination radiation as a result of increased plasma density and plasma cooling due to its expansion ($kT_e \propto 1/r^2$). The first possibility may be true in a low β plasma where magnetic field is very high and plasma expansion is low. In such a case plasma temperature should rise. But in the present experiment no change in plasma temperature was noticed in the presence of magnetic field than in the absence which rules out this possibility. The second possibility seems to be true for high β plasma where magnetic field is low. In this case confinement will be less effective and plasma after

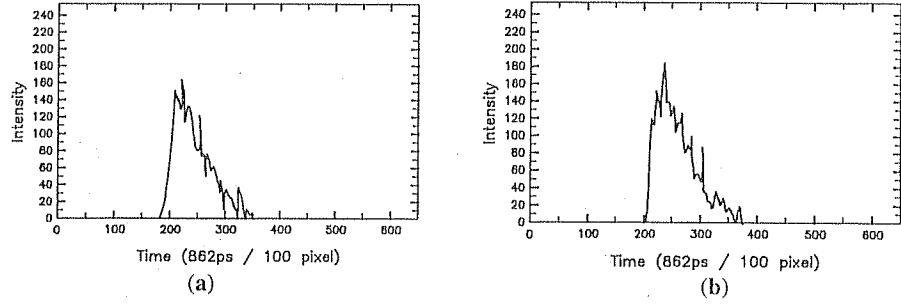


Figure 8. X-ray streak photograph. (a) In the absence of magnetic field. (b) In the presence of magnetic field.

expansion and cooling will show an enhanced recombination radiation.

A simple model and its comparison with experimental results are presented in the next section to see the effect of plasma confinement (decrease in expansion velocity) on the enhancement in x-ray emission.

4.3 Simple model for x-ray emission

A simple analysis was performed to understand the effect of an increase in density in the emission region as a result of plasma confinement that is deceleration in ion expansion. The x-ray emission from such type of plasma takes place by Bremsstrahlung, recombination and line radiation. The intensity of Bremsstrahlung radiation [26] from a plasma of volume V cm³, per unit time, in a unit frequency interval from N_e electrons/cm³ with temperature T_e interacting with N_i ions/cm³ and having effective nuclear charge state Z_i can be given by

$$\frac{dE_{\text{ff}}}{d\nu} = VCN_eN_iZ_i^2 \left(\frac{\chi_H}{kT_e} \right)^{1/2} g_{\text{ff}} \exp \left(\frac{-h\nu}{kT_e} \right). \quad (7)$$

The emission from the same volume in unit time and in a unit frequency interval due to recombination [26] into the n th shell of a hydrogen like ions of charge i is

$$\frac{dE_{\text{bf}}}{d\nu} = VCN_eN_{i+1} \left(\frac{\chi_H}{kT_e} \right)^{3/2} \left(\frac{\chi_{i,n}}{\chi_H} \right)^2 \frac{\zeta_n}{n} g_{\text{bf}} \exp \left[\frac{(X_{i,n} - h\nu)}{kT_e} \right]. \quad (8)$$

However bound-bound radiation (line radiation) is also emitted as a result of transition between bound states of the ions. The spectrum of emitted radiation therefore consists of lines at discrete wavelengths rather than being continuous. Power emitted as line radiation from a plasma of volume V cm³ is given by [27].

$$P_{\text{bb}} = 3.5 \times 10^{-25} V(kT_e)^{-1/2} N_e N_i \exp \left(\frac{-E(i)}{kT_e} \right) \text{ watt.} \quad (9)$$

Here we have considered that for the same laser intensity the coronal plasma expanding in the presence and absence of magnetic field will have nearly close plasma parameters such as plasma density, temperature and charge state Z . According to eqs (7–9) total amount

Magnetically confined laser produced plasma

of x-ray emission seems to be proportional to the volume and square of the density ($\propto N_e N_i$ where $N_e \cong N_i$) of the emitting coronal plasma. We have recorded experimentally different expansion velocity of the plasma in the absence as well as in the presence of magnetic field. Considering V_1, T_1 and V_2, T_2 as the expansion velocity and x-ray emission time in the absence and presence of magnetic field respectively where plasma expansion is spherical as has been observed in x-ray pin hole imaging [18] (figure 7). The plasma will expand a distance given by $V_1 T_1$ and $V_2 T_2$ respectively which can be considered as the radius of the hemispherical coronal plasma. If we consider $M = m\pi r^2 \tau_L$ as the mass ablated during time duration of laser (τ_L) then the plasma density can be calculated by the ratio of the mass ablated and plasma volume. Since the x-ray emission is proportional to plasma volume and density square, therefore ratio of x-ray emission in the presence (X_2) and absence (X_1) of magnetic field can be given as

$$\frac{X_2}{X_1} = \left[\frac{V_1 T_1}{V_2 T_2} \right]^3 \quad (10)$$

This indicates that x-ray emission is inversely proportional to the cube of the size (plasma expansion velocity and x-ray emission time) of the x-ray emitting coronal plasma. According to the measured dimension of plasma plume (figure 7) in the absence and presence of magnetic field as ~ 450 and $\sim 350 \mu\text{m}$ respectively, enhancement in x-ray emission $X_2/X_1 \sim 2.15$ is in close agreement with the experimental observation of 2 to 3 times increase. Putting the measured value of V_1 and V_2 as 1.4×10^7 and 1.13×10^7 cm/s respectively and $X_2/X_1 \sim 2.15$, one can get $T_1/T_2 \sim 1.03$. This shows that the x-ray emission time remains nearly ineffective of magnetic field (in the case of high β plasma) which is also in good agreement with experimental observation. The above formula obtained for the x-ray enhancement is dependent on the value of V_1/V_2 and T_1/T_2 . The dependence of V_1/V_2 on the value of plasma β is reported earlier as $V_2/V_1 = (1 - 1/\beta)^{1/2}$ [28] but variation of T_1/T_2 with β is still unknown. However, in this experiment $T_1/T_2 \sim 1$. Therefore final expression for x-ray enhancement can be written as

$$\frac{X_2}{X_1} = \left[\frac{V_1 T_1}{V_2 T_2} \right]^3 = \left[\frac{1}{(1 - 1/\beta)^{3/2}} \right] \cdot (T_1/T_2)^3 \quad (11)$$

This indicates that plasma β plays an important role in x-ray enhancement. One can conclude from this model that for high value of β enhancement in x-ray emission (the value of X_2/X_1) will be comparatively less. This conclusion seems to be in good agreement with the experimental observations presented in Figures 8a and 8b. The temporal evolution of x-ray emission measured using x-ray streak camera shows that upto 500 ps x-ray emission remains nearly same in the absence and presence of magnetic field when plasma density and temperature were high that is β is comparatively high, whereas x-ray intensity increases after 500 ps when the plasma density and temperature go down and leads a decrease in β . Results reported by Enright and Burnett also show similar variation when magnetic field was changed from 0–100 KG keeping the laser intensity constant. This indicates that plasma β will be high for a low magnetic field case where plasma density and temperature is high. But the value of β goes down as the magnetic field increases. In this experiment enhancement in x-ray intensity (X_2/X_1) was found increasing with an increase in magnetic field, that is, with decrease in plasma β . These observations are also in agreement with the prediction provided by the model. On this basis one can conclude that

the model presented here is capable of explaining the experimental observations. However better prediction is possible if the effect of β on T_1/T_2 is also known. The difference in x-ray spectrum emitted in this experiment and in Enright and Burnett experiment (100–200 keV) seems to be the characteristics of laser intensity and wavelength. This shows that enhancement in x-ray seems to be dependent mainly on β and T_1/T_2 whereas characteristics of x-rays emitted depend on type and intensity of laser used for generating the plasma. Because Enright and Burnett have used CO₂ laser in their experiment at high intensity which generated hard x-ray of high energy as well as hot electrons which is expected at higher wavelength. This indicates towards the need for a further detail study of the process of enhancement over a wide range of plasma β using different wavelength laser source along with spectroscopic diagnostics. Even the above model has further scope of improvement to get an exact idea about x-ray enhancement by including all the other possible factors responsible for x-ray emission and enhancement.

4.4 Effect of chamber pressure on x-ray emission

Figures 9a and 9b show variation in x-ray emission from laser produced plasma as the ambient pressure of the plasma chamber increases from $\sim 10^{-5}$ torr to 10^{-1} torr. Simple air was introduced in the chamber during the experiment. It was noticed that x-ray emission first decreases and then increases on both the photodiode channels as the chamber pressure increases from $\sim 10^{-5}$ to 10^{-1} torr. Similar observation has been reported earlier in the case of optical radiation from carbon plasma [29]. Measurement of ion current using Langmuir probe shows a small increase first (from 10^{-5} to 10^{-4} torr) and then a gradual decrease [30]. Ion current signal was not measurable at 10^{-1} torr using the probe located even at 5 cm distance from the target. Initial increase in ion current with pressure seems to be either due to an increase in neutral pressure and subsequent photoionization of neutrals

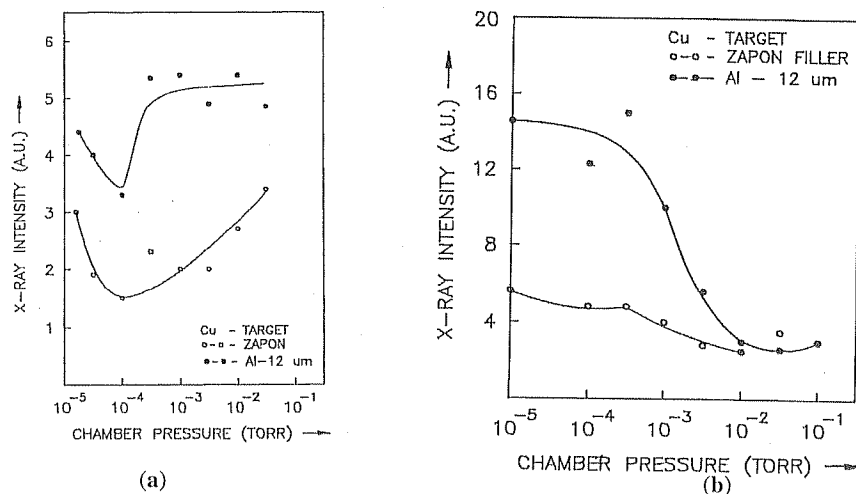


Figure 9. Variation of x-ray intensity with chamber pressure. (a). In the absence of magnetic field. (b). In the presence of magnetic field (0.6 T).

Magnetically confined laser produced plasma

due to ultra violet and x-rays produced from plasma or due to electron impact ionization of neutrals whereas further increase in pressure beyond 10^{-4} torr increases the probability of radiative as well as three body recombination. It is well known [31] that at lower densities radiative recombination is stronger than three body recombination and coronal equilibrium is established in the plasma where electron impact ionization and radiative recombination are in balance. It seems that increase in x-ray emission with increase in ambient pressure beyond 10^{-4} torr is due to enhanced radiative recombination whereas decrease in ion current seems to be due to the combined effect of radiative as well as three body recombination. However a drastic decrease in x-ray emission at very high pressure ($\sim 10^{-1}$ torr) was observed which may be due to absorption of x-rays as a result of increased population of background neutrals. It was also noticed that expansion velocity of the plasma also decreases slightly with an increase in chamber pressure. This also supports the enhancement in x-ray intensity based on the model discussed before. Figure 9b shows the variation in x-ray intensity when the ambient pressure was increased and the plasma was expanding across the magnetic field. In this case x-ray emission was maximum between $10^{-5} - 10^{-4}$ torr pressure and it started decreasing as the pressure started increasing. This observation can be explained on the basis that presence of 0.6 T magnetic field enhances the effective plasma density in emission zone even at low pressure as has been discussed earlier. However, a further increase in ambient pressure in the presence of 0.6 T magnetic field either again increases the density in the emission zone (due to pressure confinement) such that, combined effect (magnetic field and neutral pressure) starts collisional cooling of plasma or self absorption starts due to which x-ray emission goes down.

5. Conclusion

In summary we can say that the biplanar photodiode developed to study the x-ray emission is operating successfully. Its design is very simple so that it can be made in any laboratory.

X-ray emission study from a laser produced plasma expanding across a magnetic field shows that x-ray emission got enhanced by 2–3 time in the presence of 0.6 T magnetic field. A simple analytical model supports the experimental observations of x-ray enhancement and temporal evolution of x-ray emission from laser produced plasma expanding in magnetic field. Enhancement in x-ray emission seems to be due to enhanced recombination radiation after ~ 500 ps as a result of increased plasma density due to magnetic confinement and decreased temperature as a result of plasma expansion. Even x-ray emission increases and expansion velocity decreases with an increase in ambient chamber pressure up to a certain pressure as a result of confinement due to neutral pressure. Here again enhancement seems to be due to increased radiative recombination like the magnetic confinement case.

Although the present experiment was performed for a fixed magnetic field but it could provide a picture of x-ray enhancement for a wide value of plasma β as a result of x-ray streak camera measurement except the effect of laser wavelength on it. This indicates towards a further detailed experimental study for various β values, along with x-ray spectroscopic diagnostics and using different wavelength lasers for producing the plasma. Even the analytical model also has a scope of improvement by considering various other factors affecting x-ray emission.

Important finding of this experiment was that presence of dc magnetic field generates many interesting effects in laser produced plasma such as enhancement in x-ray emission,

generation of instability as well as high energy x-rays along with some fast ions out of which x-ray enhancement will have good application in inertial confinement fusion experiments [28].

Acknowledgment

Authors are thankful to D D Bhawalkar for helpful suggestions. S R Shinde is gratefully acknowledged for providing ferrite magnet for these experiments.

References

- [1] A A Hauer and H A Baldis, *Laser induced plasmas and applications*, edited by L J Radziemski and D A Cremers (Marcel Dekker, Inc. New York, 1989)
- [2] D A Attwood, *IEEE. J. Quant. Electron* **QE14**, 909 (1978)
- [3] G Beck, *Rev. Sci. Instrum.* **47**, 849 (1976)
- [4] F P Adams, A Ng and Y Gazit, *Rev. Sci. Instrum.* **58**, 1130 (1987)
- [5] C J Armentrout, J B Geddes, P Lee and L R Canfield, *Rev. Sci. Instrum.* **59**, 1843 (1988)
- [6] R Sauneuf, *SPIE* **1140**, 466 (1989)
- [7] M Shukla, V N Rai, S N Pisharody and H C Pant, *Proc. of National Laser Symposium CAT*, Indore 6-8 Feb. (1997) pp 147
- [8] V N Rai, M Shukla and H C Pant, *Proceedings national laser symposium*, IRDE Dehradun, 10-14 Feb. (1995) pp. 269
- [9] J F Drake, P K Kaw, Y C Lee, G Schmidt, C S Liu and M N Rosenbluth, *Phys. Fluids* **17**, 778 (1974)
- [10] D F Forslund, J M Kindel and K Lee, *Phys. Rev. Lett.* **39**, 284 (1977)
- [11] B Yaakobi, P Bourke, Y Conturie, J Delettrez, J M Forsyth, R D Frankel, L M Goldman, R L McCrory, W Seka, J M Soures, A J Burek and R E Deslattes, *Opt. Commun.* **38** 196 (1981)
- [12] J E Balmer and T P Donaldson, *Phys. Rev. Lett.* **39**, 1084 (1977)
- [13] M C Richardson, R Epstein, O Barnouin, P A Jaanimagi, R Keck, H G Kim R S Mayoribanks, S Noyes, J M Soures and B Yaakobi, *Phys. Rev.* **A33**, 1246 (1986)
- [14] J E Balmer, R Weber, P F Cunningham and P Ladrach, *Laser and particle beams* **8**, 327 (1990)
- [15] S Suckewer and H Fishman, *J Appl. Phys.* **51**, 1922 (1980)
- [16] S Suckewer and H Skinner, H Milchberg, C Keane and D Noorhees, **55**, 1753 (1985)
- [17] G D Enright and N H Burnett, *Phys. Fluid* **C29**, 3456 (1986)
- [18] V N Rai, M Shukla and H C Pant, *Recent advances in plasma science and technology*, edited by R P Singh, S B Rai and D Narayan (Allied Publishers Ltd. New Delhi, 1996) pp. 191
- [19] V N Rai, M Shukla, H C Pant and D D Bhawalkar, *Sadhana: Academy proceeding in engineering sciences* **20**, 937 (1995)
- [20] V N Rai, M Shukla and H C Pant, *Proc. National symposium on plasma science* edited by P K Gosh (Prentice Hall of India Pvt. Ltd., New Delhi, 1996) pp. 118
- [21] R D Bleach and D J Nagel, *J. Appl. Phys.* **49**, 3832 (1978)
- [22] D Sydora, J S Wagner, L C Lee, E M Wescott and T Tajima, *Phys. Fluid* **26**, 2986 (1983)
- [23] C T Chang and M Hashmi, *Phys. Fluid* **20**, 533 (1977)
- [24] R G Tuckfield and F Schwirzke, *Plasma physics* **11**, 11 (1969)
- [25] D K Bhadra, *Phys. Fluid* **11**, 234 (1968)
- [26] R H Huddleston and S L Leonard, *Plasma diagnostics technique* (Academic Press, New York, 1965)
- [27] H R Griem, *Plasma Spectroscopy* (Mc Graw Hill, New York, 1964)
- [28] S Yu Guškov, T Pisarczyk and V B Rozanov, *Laser and particle beam* **12**, 371 (1994)

Magnetically confined laser produced plasma

- [29] R K Dwivedi and R K Thareja, *Phys. Rev.* **B51**, 7160 (1995)
- [30] V N Rai, M Shukla and H C Pant, *National laser symposium IRDE*, Dehradun 10-14 Feb (1995)
- [31] R J Goldston and P H Rutherford, *Introduction to plasma physics*, (Institute of Physics Publishing, Bristol, Philadelphia, 1995)

